Do resident thyroid stem cells have a role in regeneration of hypophyseal thyroid axis after experimentally induced hypothyroidism in male rats? A histological and immunohistochemical study

Manal M. Shehata[a], Nashwa A. M. Mostafa[a], Alaa M. Metwally[a], Asmaa M. S. Gomaa[b]

Departements of [a]Histology and Cell Biology, [b]Medical Physiology, Faculty of Medicine, Assiut University, Assiut, Egypt

Correspondence to Alaa M. Metwally, Kbaa Street from El Glaa Street, Assiut, Egypt. Zip Code: 71515; 01017422334; e-mail: alaasayed255212@yahoo.com

Received 21 November 2020
Revised 30 December 2020
Accepted 01 January 2021
Published 09 October 2021

Journal of Current Medical Research and Practice
2021, 6:247–256

Background
Hypothyroidism is a common endocrine disorder characterized by a deficiency of thyroid hormones less than the normal levels. Recent research studies identified the presence of stem cells that act as a source of tissue regeneration within the thyroid gland.

Aim
To investigate the role of resident thyroid stem cells on the hypophyseal thyroid axis in experimentally induced hypothyroidism in male rats.

Materials and methods
A total of 30 healthy male rats were randomly divided into three groups. Group I was the control group). Group II was the hypothyroid group. It received carbimazole in a dose of 0.6 mg/kg dissolved in water to induce hypothyroidism. It was administered via an orogastric tube daily for 3 months. Group III was the withdrawal group. It included hypothyroid animals, as in group II, that were left without treatment for another month and then killed to assess hypothyroidism's recovery. The thyroid and pituitary glands were extracted from all groups and processed for histological and immunohistochemical analysis.

Results
The present study revealed that hypothyroidism caused marked histological changes in the pituitary–thyroid axis. Shrunken thyroid follicles with a significant increase in the epithelial height were seen. The colloid decreased in follicles or was completely absent in others. The follicular cells showed vacuolated cytoplasm. A significant increase in the number of parafollicular cells was observed. Thyrotrophs also appeared vacuolated with an increase in their number. Increase in the apoptotic cells and vascular endothelial growth factor-immunostained cells were observed. The withdrawal group showed moderate improvement in the architecture of the thyroid and pituitary glands. These results were confirmed by the morphometric and thyroid function test analysis.

Conclusion
The presence of resident thyroid stem cells led to moderate thyroid structure improvement but was not sufficient to restore the normal thyroid function.

Keywords:
hypothyroidism, parafollicular cells, pituitary, stem cells, thyroid gland

J Curr Med Res Pract 6:247–256

2357-0121

Introduction

The thyroid gland controls energy usage, metabolism, and protein synthesis [1]. The pituitary gland is the 'master gland,'which is involved in most body functions' homeostatic regulation. The thyroid gland activity is under the control of the hypothalamic–pituitary–thyroid axis [2].

Hypothyroidism is a frequent thyroid dysfunction characterized by low production of thyroid hormones. Hypothyroidism leads to impairments in many organs [3].

The thyroid gland is characterized by slow turnover. It divides only five times in human adult and animals, like dogs, rats, and mice. Cell division and cell death compensate each other. The thyroid gland can grow in response to a stimulus through cell hypertrophy and proliferation [4].

Adult stem cells are present in many tissues. They are responsible for the repair and regeneration of the tissue after injury [5]. A few authors have studied resident adult stem cells of the human thyroid because

hypothyroid patients can be treated with standardized levothyroxine therapy. This hormone was used to produce the molecule secreted by the gland [6].

Although some authors have suggested the existence of stem cells in the thyroid, but how these cells participate in thyroid regeneration is still unclear [7]. So, our work aimed to evaluate the role of these stem cells in the regeneration of the hypophyseal thyroid axis in experimentally induced hypothyroidism in male rats.

Materials and methods

This study was done in Assiut University, Assiut Faculty of Medicine approved the study, with IRB no. 17101204.

Animals

A total of 30 healthy male rats were used. Their weight was 180–200 g. They were purchased from the Animal House, Faculty of Medicine, Assiut University. Ethical approval was provided by the medical ethics committee, Faculty of Medicine, Assiut University.

Experimental design

The rats were randomly divided into three groups:

(1) Group I (GI): it included ten rats that received distilled water (0.5 ml for each rat), orally via an orogastric tube.
(2) Group II (GII): it included ten rats that received carbimazole to induce hypothyroidism at a dose of 0.6 mg/kg dissolved in 50 ml of water daily via an orogastric tube for 3 months [8,9], and then killed.
(3) Group III (GIII): it included ten hypothyroid animals that were left without treatment for another month, and then killed to assess the recovery from hypothyroidism.

Biochemical study

Before killing, retro-orbital blood samples were collected and then centrifuged at 3000 rounds per min for 15 min. The clear, nonhemolyzed supernatant sera were removed and kept at −20°C until use for the assessment of the levels of total T3, total T4, and thyroid-stimulating hormone (TSH) using enzyme-linked immunosorbent assays commercial kits (BioSource, Europe, Belgium) according to the instructions of each kit [10].

Histological study

At the end of 3 months for GI and GII and 4 months for GIII, rats were anesthetized by ether inhalation. Thyroid and pituitary glands were removed and processed for the following:

(1) For light microscopic study: after fixation in 10% buffered formalin solution, the samples were processed to prepare paraffin sections that were stained by hematoxylin and eosin and periodic acid Schiff (PAS) [11].

For immunohistochemical staining: thyroid sections were stained using anticalcitonin to detect parafollicular cells and Oct-4 to detect resident stem cells. Pituitary sections were stained using TSH antibody to detect thyrotrophs. Thyroid and pituitary sections were stained using an anti-vascular endothelial growth factor (VEGF) antibody to detect angiogenesis, vasculogenesis, and endothelial cell growth and anti-caspase-3 antibody to detect apoptosis [11]. All immunostaining methods used produced cytoplasmic reactions.

For electron microscopic study: small specimens were taken from the thyroid and pituitary glands and were immediately fixed in 5% phosphate buffered glutaraldehyde at 4°C for 24 h and postfixed in 1% osmium tetroxide for 2 h. Embedding was done in Epon (TAAB-812; Embedding Resin Kit, England, London) 812. Semithin sections (l μm) were cut, stained with toluidine blue, and examined by light microscopy. Ultrathin sections (50–80 nm) from the selected areas were contrasted with uranyl acetate and lead citrate [12] and were examined in transmission electron microscopy (J. E. M. 100 CXII, Tokyo, Japan) and photographed at 80 kV at Assiut University Electron Microscopy Unit.

Morphometric analysis

The diameter and epithelial height of the thyroid follicles were measured at a magnification of ×400. The area percentage of colloid in PAS-stained slides in the thyroid was measured at a magnification of ×400. The numbers of calcitonin immunoreactive C cells and Oct-4-positive cells in the thyroid parenchyma, caspase-3-positive cells in the thyroid and pituitary glands, and positively stained thyrotrophs were measured at magnification of ×1000. The area percentage of VEGF-positive reaction in the thyroid and pituitary glands was measured at magnification of ×1000.

Measurements were done in 10 nonoverlapping fields for each rat (Leica Qwin 500; Leica, Cambridge, UK) in the Histology Department, Faculty of Medicine, Assiut University.

Statistical analysis

The morphometric and biochemical measurements were expressed as mean ± SD and were analyzed

statistically using one-way analysis of variance followed by 'Tukey' post-hoc test. Analyses were done using SPSS software, version 16 (SPSS Inc., Chicago, Illinois, USA). Results were considered significant when the *P* value was less than 0.05 [13].

Results

General observation

No deaths were observed in rats during the experiment.

Histological results

(1) The thyroid gland:
   (a) Light microscopic results:

In GI, the thyroid gland revealed multiple follicles lined with cuboidal epithelium and filled with uniformly acidophilic colloid. The follicular epithelium was formed of follicular cells-contained vesicular nuclei and parafollicular (C) cells. Parafollicular cells had oval vesicular nuclei and lightly stained cytoplasm present between follicular cells and basement membrane and not reaching the follicular lumen (Fig. 1a). In GII, there was a distortion of the follicular architecture. Multiple thyroid follicles appeared reduced in size with highly vacuolated cytoplasm. Some follicles were filled with a scanty colloid, and others were completely devoid of colloid. Congested dilated blood capillaries were observed among the follicles (Fig. 1b). In GIII, the cells appeared less vacuolated. Desquamated epithelial cells were frequently noticed. Dilated congested blood capillaries were observed (Fig. 1c).

With PAS staining: GI showed a prevalent PAS-positive reaction in the colloid and the basement membranes (Fig. 1d). GII demonstrated multiple follicles with widespread PAS-negative reaction in their lumen and PAS-positive reaction in the basement membrane, which appeared discontinuous in some follicles (Fig. 1e). GIII showed PAS-positive reaction in the colloid with a negative reaction in the vacuoles in many follicles (Fig. 1f).

Using anticalcitonin immunostaining, GI revealed a positive cytoplasmic reaction in C cells (Fig. 2a), GII showed an increase in the number of positive C cells (Fig. 2b), and GIII showed that immunoreactive C cells were less than GII (Fig. 2c).

Figure 1

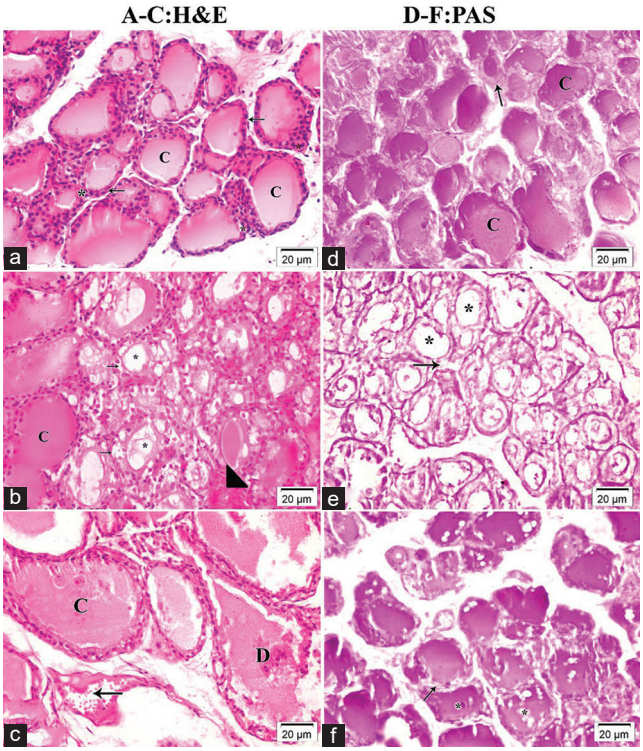

(a) GI follicular cells (→), Cells (*) and colloid (c). (b) GII vacuolated follicular cells (→) with no colloid (*) others have colloid (c). Congested capillaries (►). (c) GIII with desquamated cells (d), colloid (c), and congested capillaries (→). (d) GI, a ve + reaction in colloid (c) and basement membrane (→). (e) GII with a – ve reaction in lumina (*) and discontinuous reaction in basement membrane (→). (f) GIII ve + reaction of colloid and – ve in the vacuoles (*). Basement membrane is ve + stained (→). (a–c) H and E × 400. (d–f) PAS × 400. H and E, hematoxylin and eosin; PAS, periodic acid Schiff.

Figure 2

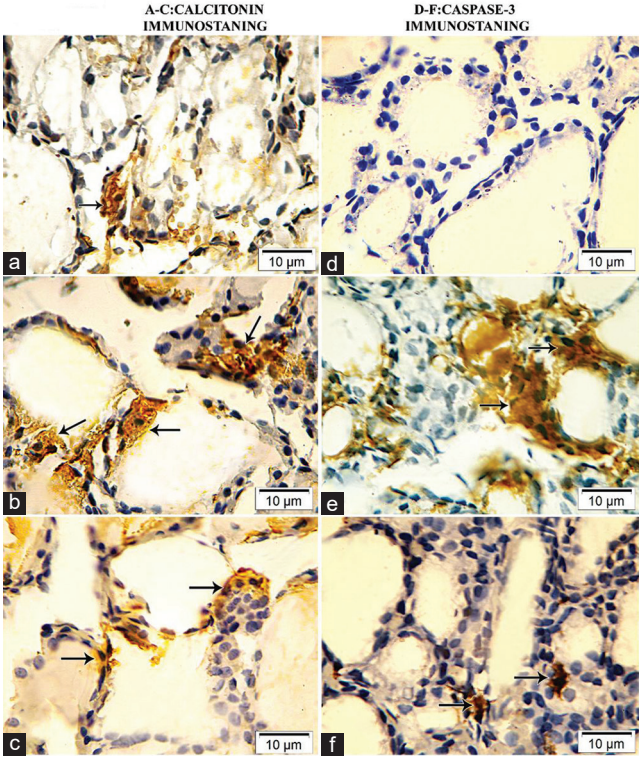

(a) GI, with positive reaction for calcitonin in C cells (→). (b) GII showing increase in the positive C cells (→). (c) GIII showing groups of immunoreactive C cells are observed (→) but they are less than group II. (d) GI, showing a negative reaction for caspase-3. (e) GII showing a highly positive reaction (→) in many cells. (f) GIII, showing that positive cells are observed in the follicles but they are less than GII (→). (a–c) calcitonin immunostaining × 1000. (d–f) caspase-3 immunostaining × 1000.

Using anticaspase III immunostaining: in GI, a negative reaction was observed (Fig. 2d); in GII, a highly positive cytoplasmic reaction appeared in many cells (Fig. 2e); and in GIII, positive cells were observed in the follicles, but they were less than GII (Fig. 2f).

Using anti-VEGF immunostaining: in GI, a positive immunostaining for VEGF in the endothelial cells lining the blood vessels was observed (Fig. 3a); in GII, an increase in the positive reaction was noticed (Fig. 3b); and in GIII, a decrease in the positive reaction was observed compared with GII (Fig. 3c).

Using anti-Oct-4 immunostaining: GI revealed a few immunostained cells among the follicles (Fig. 3d); in GII, many immunostained cells were noticed (Fig. 3e); and GIII showed a few immunostained cells (Fig. 3f).

(b) Electron microscopic results:

GI: semithin sections revealed that the follicles were lined with cuboidal follicular cells. Ultrastructurally, the thyroid follicular cells were cuboidal and possessed rounded euchromatic nuclei and abundant rER in the cytoplasm. Their apices were characterized by numerous irregular microvilli projected into the follicular lumen that contained an electron-dense colloidal substance. Numerous mitochondria and lysosomes were observed. Tight junctions were observed at the apical margins of opposing cells (Fig. 4a).

Semithin sections showed that the parafollicular cells appeared larger, paler, and not reaching the follicles' lumen. Ultrastructurally, parafollicular cells appeared single or in groups. They had euchromatic nuclei, and their cytoplasm contained numerous granules, mitochondria, and short rER cisternae (Fig. 4b).

Figure 3

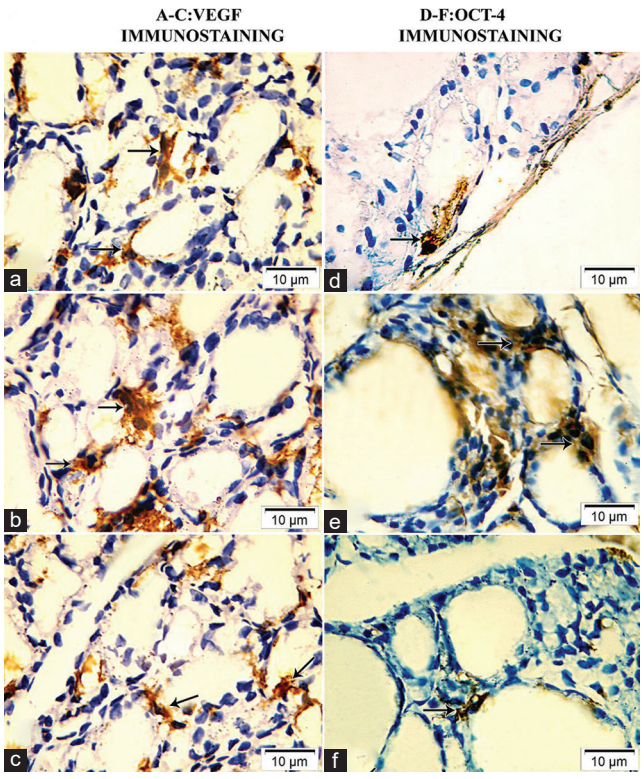

(a) The thyroid gland of GI, showing a positive reaction for VEGF in the endothelial cells lining the blood vessels (→). (b) In GII, an increase in the positive reaction is observed (→). (c) In GIII, a decrease in the reaction compared to group II (→). (d) GI, showing that few positive cells of Oct-4 are observed among the follicles (→). (e) In GII, many positive cells are observed (→). (f) In GIII, few positive cells (→) are observed. (a–c) VEGF immunostaining. (d–f) Oct-4 immunostaining. VEGF, vascular endothelial growth factor.

Figure 4

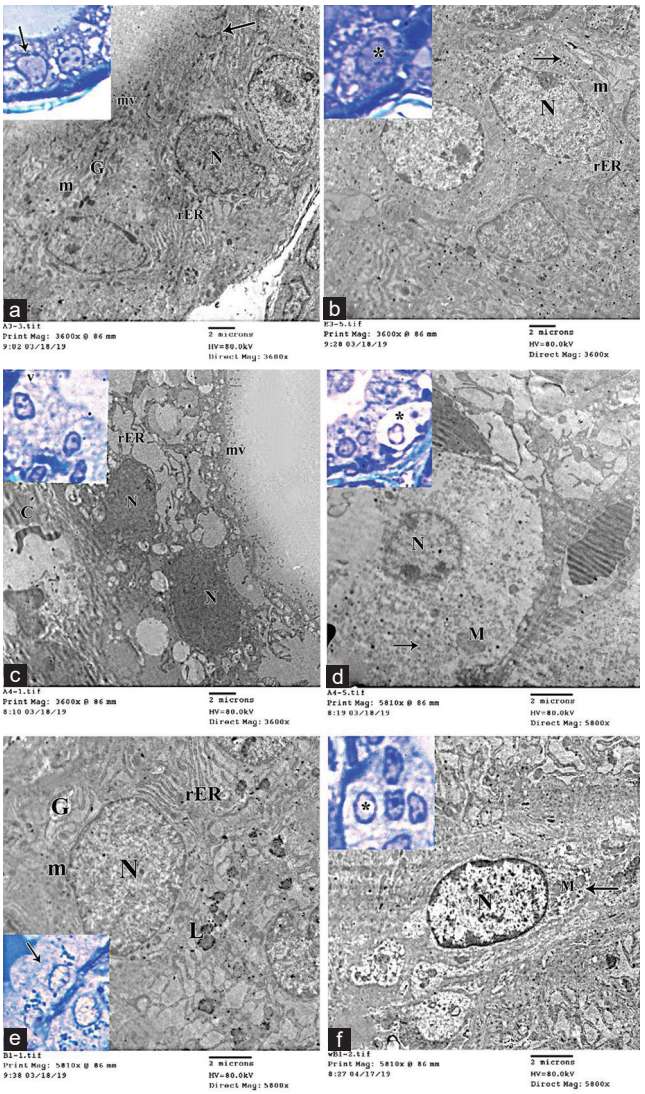

(a) Inset: GI follicular cells→. EM: nuclei (N), rER, microvilli (mv), mitochondria (m), Golgi (G) and junction→. (b) Inset: GI C cells (*). EM: nucleus (N), granules→, mitochondria (m) and rER. (c) Inset: GII vacuolated cells (V). EM: irregular nuclei (N), swollen rER, microvilli (mv) and congested vessels (c). (d) Inset: GII with vacuoles (*). EM: nucleus (N), granules → and mitochondria (m). (e) Inset: GIII less vacuoles. EM: nucleus (N), dilated Golgi (g), dilated rER, lysosomes (L) and mitochondria (m). (f) Inset: GIII C cells (*). EM: nucleus (N), mitochondria (M) and granules→. Inset: TB × 1000. EM: (a–c) ×3600 and (d–f) ×5800. TB, toluidine blue.

GII semithin sections showed that follicular cells had vacuolated cytoplasm. Ultrastructurally, many thyroid follicular cells appeared with irregular hyperchromatic nuclei. Their cytoplasm showed a swollen ER, several large vacuoles, dilated mitochondria in the cytoplasm, and a small number of microvilli. The basement membrane was ill-defined. Congested blood vessels in the interfollicular tissue were observed (Fig. 4c).

Semithin sections showed parafollicular cells with highly vacuolated cytoplasm. They had small irregular apoptotic nuclei and rarified cytoplasm that contained electron-dense granules (Fig. 4d).

GIII semithin sections showed that the follicular cells had mild vacuolation. Ultrastructurally, the follicular cells-contained euchromatic nuclei, and their cytoplasm had fewer vacuoles, less dilated rER, and Golgi bodies. Many lysosomes could be seen (Fig. 4e).

Semithin sections showed parafollicular cells with mild vacuolation. Ultrastructurally, they had oval nuclei with peripheral heterochromatin. The perinuclear space was dilated. They contained few vacuoles, mitochondria, and few secretory granules (Fig. 4f).

(2) The pituitary gland:

(a) Light microscopic results:

In GI, the pars distalis revealed irregular cords of cells separated by fenestrated blood capillaries. Two types of cells were present: chromophobes and chromophils. Chromophils were large cells that were subdivided into acidophils (A) and basophils (B) (Fig. 5a). In GII, marked vacuolation of chromophobes was seen. Many chromophils had irregular outlines with deeply stained irregular nuclei and deeply stained acidophilic cytoplasm. Dilated congested blood capillaries were observed (Fig. 5b).

In GIII, vacuolated cells and deeply stained chromophils were less observed compared with GII (Fig. 5c).

Using anti-TSH immunostaining: in GI, TSH-immunopositive cells were observed (Fig. 6a). In GII, TSH-immunopositive cells were significantly increased compared with GI (Fig. 6b). In GIII, TSH-immunopositive cells were decreased in number compared with GII (Fig. 6c).

Using anti-caspase-3 immunostaining: in GI, there were few faint positively stained cells (Fig. 7a). In GII, a significant increase in the positive cells was observed (Fig. 7b). In GIII, there were many positive cells but less than GII (Fig. 7c).

Using anti-VEGF immunostaining: GI showed a few immunostained cells in blood vessels' wall (Fig. 7d). In GII, a significant increase in the positive reaction was observed (Fig. 7e). In group GIII, a marked decrease in the positive reaction was observed (Fig. 7f).

Figure 5

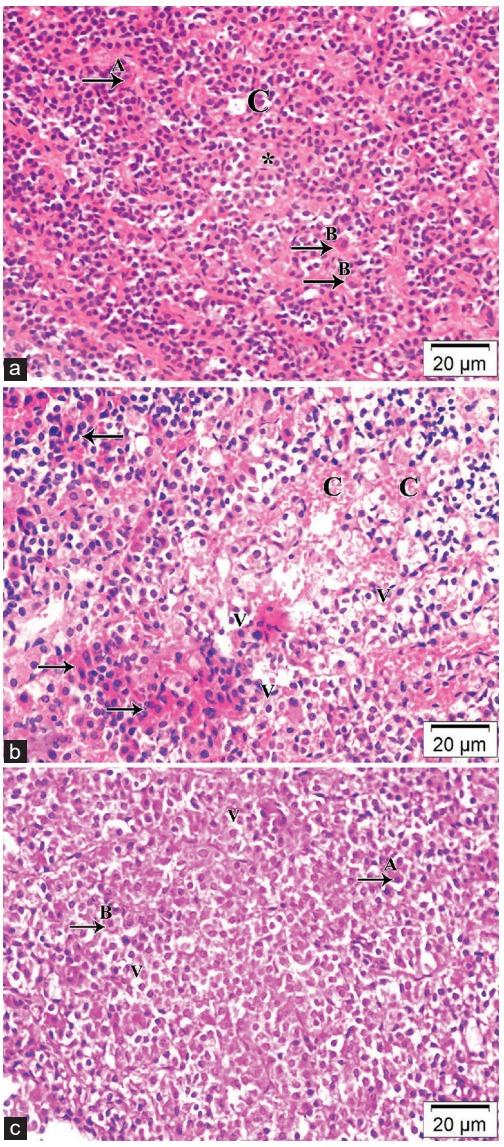

(a) The pars distalis of GI showing irregular cords of cells; chromophobes (*) and chromophils : acidophil (A) and basophil (B) separated by blood capillaries (c).(b) GII showing marked vacuolation of chromophobes (V). Many chromophils exhibit irregular outlines with deeply stained cytoplasm and nuclei (→). Dilated congested capillaries are observed (C). (c) GIII showing that vacuolated cells are still observed (V) but less than GII. Notice, acidophil (A) and basophil (B). H and E × 400. H and E, hematoxylin and eosin.

(b) Electron microscopic results:

In GI, semithin sections showed that the thyrotrophs were small branched cells. Ultrastructurally, they were distinguished by their small size, angular shape, and cytoplasmic processes. Their cytoplasm is characterized by small electron-dense secretory granules distributed in the periphery along the plasma membrane. Oval or rounded mitochondria and rER were observed (Fig. 8a).

Figure 6

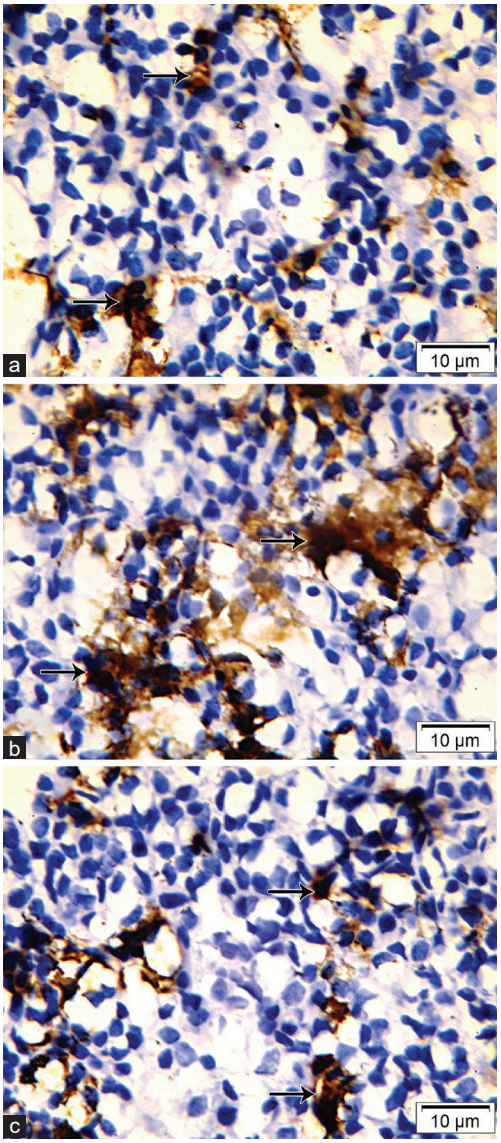

(a) The pars distalis of GI showing TSH-immunopositive cells (→). (b) GII showing that TSH-immunopositive cells are highly increased in number (→). (c) GIII showing that TSH-immunopositive cells decrease in number compared to GII (→). TSH immunostaining × 1000.

In GII, semithin sections showed that the thyrotrophs had deeply stained cytoplasm with irregular deeply stained nuclei. Ultrastructurally, thyrotrophs revealed irregular nuclei with peripheral heterochromatin and dilated perinuclear space. The cytoplasm was vacuolated, which may be due to dilated rER cisternae engorged with secretion. These cells were irregular with ill-defined borders. The cytoplasm of these cells had many electron-dense secretory granules distributed throughout the cytoplasm (Fig. 8b).

In GIII, semithin sections showed that thyrotrophs had lightly stained cytoplasm and nucleus. Ultrastructurally, they had rounded euchromatic nuclei and contained many secretory granules with different electron densities. There was a marked decrease in the cytoplasmic vacuolations (Fig. 8c).

Figure 7

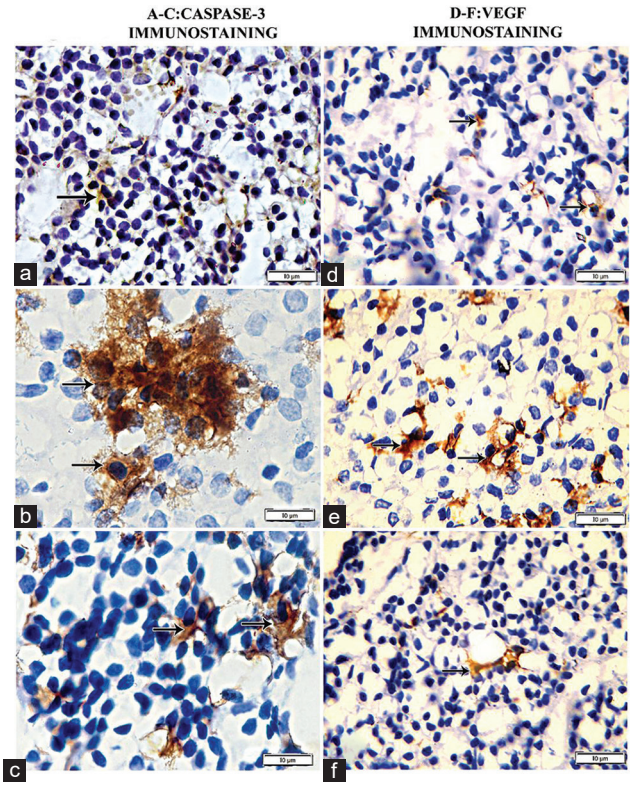

(a–c) Caspase immunostaining. (d–f) VEGF immunostaining. (a) Pars distalis of GI showing that there are few faint positively stained caspase-3 cells (→). (b) GII showing that there is marked increase in the positive cells (→). (c) GIII showing that there are positive cells but less than GII (→). (d) Pars distalis of GI, showing few positive cells of VEGF in the wall of blood vessels (→). (e) GII, showing increase in the positive reaction (→). (f) GIII, showing marked decrease in the positive reaction (→). VEGF, vascular endothelial growth factor.

Biochemical results

In GII, serum values of both T3 and T4 were significantly decreased (0.62 ± 0.01 and 5.58 ± 0.31, respectively) when compared with GI (1.26 ± 0.06 and 12.01 ± 0.15, respectively) and were significantly increased in GIII (1.03 ± 0.01 and 9.62 ± 0.46, respectively) versus GII (Fig. 9a and b). In contrast, the mean value of TSH was significantly increased in the GII (2.33 ± 0.19) than GI (0.73 ± 0.06) and decreased in GIII (0.53 ± 0.01) in comparison with GII (Fig. 9c).

Morphometric results

(1) The mean values of follicular diameter are significantly decreased in GII compared with GI and a significant increase in GIII compared with GII (Fig. 10a).
(2) The mean values of follicular epithelial height are significantly increased in GII compared with GI and significantly decrease in GIII compared with GII (Fig. 10b).
(3) The mean area percentage of colloid in GII showed a significant decrease compared with GI, and a significant increase in GIII compared with GII (Fig. 10c).

Figure 8

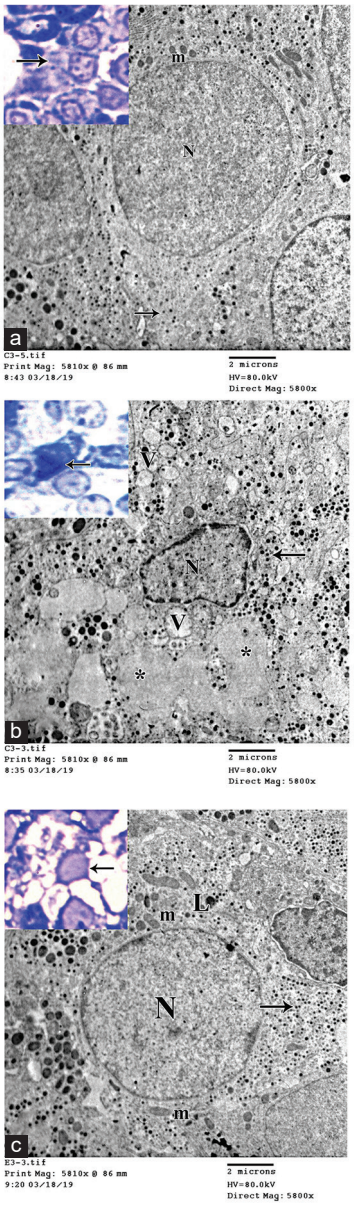

(a) Inset: GI branched thyrotroph (→). EM: it contains electron-dense granules(→), mitochondria (m) and nucleus (N). (b) Inset: GII thyrotroph has deeply cytoplasm and nucleus (→). EM thyrotroph with apoptotic nuclei (N), contains many electron-dense granules (→) and cytoplasmic vacuoles (V), may be dilated rER (*). (c) Inset: GIII thyrotroph with lightly stained cytoplasm and nucleus (→). EM thyrotroph has rounded nuclei (N), many secretory granules (→), lysosomes (L) and mitochondria (m). Inset: TB × 1000. EM: ×5800. TB, toluidine blue.

Figure 9

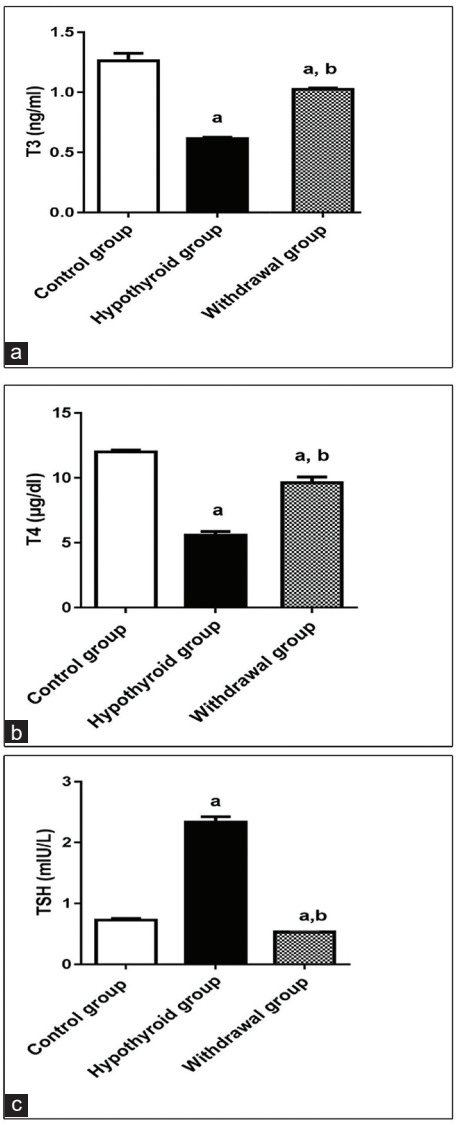

(a) Serum levels of T3 in rats (ng/ml). (b) Serum levels of T4 in rats (µg/dl). (c) Serum level of TSH in rats (mIU/l).

(4) The mean number of calcitonin immunopositive cells was significantly increased in GII in the thyroid and pituitary glands compared with GI, whereas in GIII was significantly decreased compared with GII (Fig. 10d).
(5) The mean number of caspase-3 immunopositive cells was increased in the GII and GIII compared with GI (Fig. 10e).
(6) The mean number of Oct-40positive cells (Fig. 10f) and positively-stained thyrotrophs (Fig. 10g) was significantly increased in GII compared with the other groups.
(7) The area percentage of VEGF-positive reaction in the thyroid and pituitary glands was significantly increased in GII compared with other groups (Fig. 10h).

Discussion

The thyroid gland has an essential function in producing thyroid hormones that act on almost all tissues' cells and therefore are necessary for many physiological processes in the body [14].

Our study was done to elucidate resident thyroid stem cells' role after the withdrawal of carbimazole drug in an experimental model of hypothyroidism

Figure 10

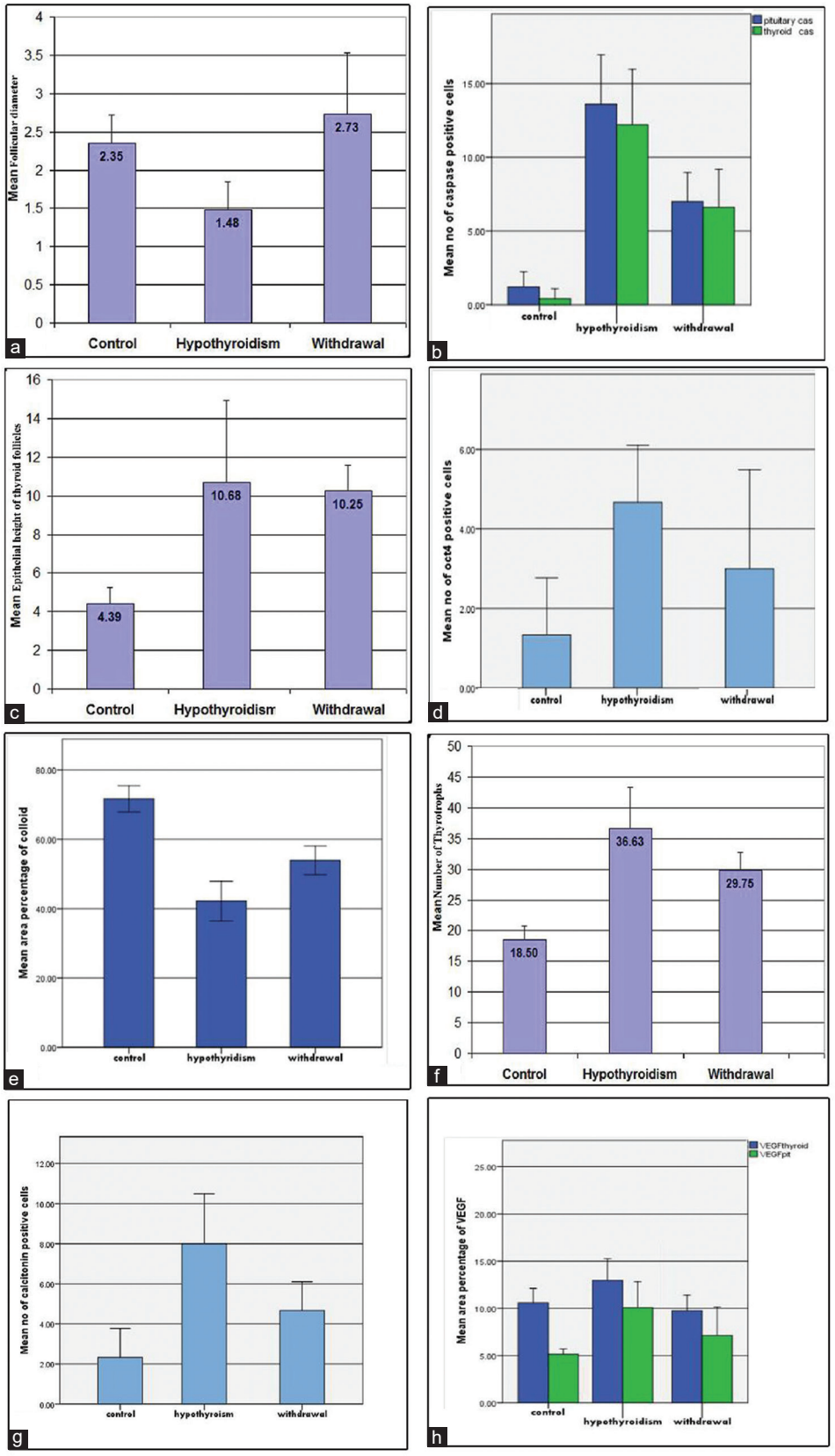

(a).Mean follicular diameter in different groups. (b) Mean epithelial height of thyroid follicles in different groups. (c) Mean area percentage of colloid in different groups. (d) Mean number of calcitonin positive cells in different groups. (e) Mean number of caspase-3-positive cells in different groups. (f) Mean number of Oct-4-positive cells in different groups. (g) Mean number of thyrotrophs in different groups. (h) Mean area percentage of VEGF in different groups. VEGF, vascular endothelial growth factor.

in male albino rats. Carbimazole was the drug of choice for the induction of hypothyroidism because it was widely available, cost-effective, and noncytotoxic [15].

In GII, there was marked histological alteration in the structure of the thyroid and pituitary glands. The follicular cells appeared vacuolated, and the follicles decreased in size with a decrease in the volume of colloid up to a complete absence of colloid in some follicles. There was a significant increase in the number of C cells. Thyrotrophs also appeared vacuolated with an increase in their number. An increase in the apoptotic cells and VEGF-positive cells was observed. These results were confirmed by the morphometric and thyroid function test analysis.

We explained these results by degenerative changes that occurred owing to carbimazole and some follicles' collapse owing to colloid diminution from the lumen [16].

Our results were in line with other researchers [17] who clarified that hypothyroidism in dogs led to the degeneration of individual follicular cells, and also others [18] observed degeneration of follicular cells, with some abnormal changes owing to chlorpyrifos insecticide-treated rats, demonstrated hypothyroidism. These changes were explained due to the inhibition of iodide taken at the sodium iodide symporter of the thyroid gland owing to decreased thyroglobulin synthesis [19].

In our study, the endoplasmic reticulum was markedly dilated. It was clarified that rER played a vital role as it was essential in the synthesis of thyroglobulin and thyroid peroxidases. The mechanism of action of the antithyroid drug was the inhibition of peroxidases resulting in lowered TH levels [20]. Moreover, we observed multiple congested blood vessels. The congestion was owing to the inflammatory process with carbimazole [21].

Our work showed histological alternations in C cells in GII. Besides a significant increase in their number, they appeared hypertrophied, with small irregular nuclei, swollen mitochondria, and rarified cytoplasm. These findings denoted the possibility of communication between the follicular and the parafollicular cells. We suggested that the changes in C cells coincided with the changes in the follicular cells. These results coincide with other authors who demonstrated that hyperactivity in C cells as in follicular cells might be because of the high TSH hormone level, leading to hyperplasia and hypertrophy of the parafollicular cells [22,23].

We declared that the histological alteration found in the pituitary gland was secondary to thyroid changes. Our findings agreed with Diaz-Espineira *et al.* [24], who studied changes in dogs' pituitary, and detected morphological alternations in the adenohypophysis with primary induced hypothyroidism and found many large pale cells with vacuoles throughout the adenohypophysis area. Hyperplasia of thyrotrophic cells was due to the loss of thyroxine hormone, which led to feedback inhibition and overproduction of thyrotropin-releasing hormone [25].

In GIII, there was a moderate improvement in the architecture of the thyroid and pituitary glands. The follicular cells appeared less vacuolated with more colloid compared with the group II. C cell numbers were significantly decrease. Thyrotrophs also appeared less vacuolated with a decrease in their number. A decrease in the apoptotic cells and VEGF-positive cells was observed compared with GII. These results were confirmed by the morphometric and thyroid function test analysis.

Our results explained this improvement in the thyroid gland structure owing to the presence of resident thyroid stem cells. We confirmed the presence of these cells by Oct-4-positive immunostaining. We found a decrease in their number in GIII, and this is explained by the exhaustion of these cells in the regeneration of thyroid tissue. The improvement in the structure of the pituitary gland was secondary to thyroid gland regeneration.

Our results were in line with other authors who recognized and characterized adult stem resident in different organs. They elucidate that these cells are accountable for tissue renewal and regeneration after injury [26,27]. More recently, results in stem cell biology have furnished proof for the presence of adult stem cell populations (resident SSCs) within the human and mouse thyroid [28,29]. Adult/stem cells were first isolated from the mouse thyroid [30,31].

Other authors clarified this improvement by the capability of some follicular cells to recover some of the original structure on the drug's stoppage [32]. When stress decreased and declined in the form of stoppage of the drug, they found that involution appeared, the epithelial height decreased, colloid accumulated, and follicular cells resumed their average size and shape [32].

We found that the improvement in the thyroid gland structure was not sufficient to restore the normal structure. We explained this that stem cells resident in different organs have a limited differentiation

potential, showing the capacity to produce mature cells of the tissue of origin but may also transdifferentiate to produce multiple specialized cell types. Instead, a low division rate of endogenous stem cells was seen [33]. Moreover, to remain undifferentiated, these cells need to be protected in a specific microenvironment: the niche [34].

Financial support and sponsorship
Nil.

Conflicts of interest
There are no conflicts of interest.

References

1 Elazeem AA, Mohammed MZ, Hassan EZ. Effect of experimentally induced hypothyroidism on the parotid gland of adult male albino rats and the possible role of thyroid hormone supplementation. Br J Sci 2016; 1:14.

2 Davis SW, Castinetti F, Carvalho LR, Ellsworth BS, Potok MA, Lyon RHS, *et al*. 'Molecular mechanisms of pituitary organogenesis: In search of novel regulatory genes. Mol Cell Endocrinol 2010; 323:4–19.

3 Selim SA, Alazouny ZM. The effect of experimental hypothyroidism on the skin of adult male albino rats and the therapeutic role of topical triiodothyronine: a histological and immunohistochemical study. Egypt J Histol 2015; 38:649–658.

4 Dumont JD, Lamy F, Roger PC, Maenhaut C. Physiological and pathological regulation of thyroid cell proliferation and differentiation by thyrotropin and other factors. Physiol Rev 1992; 72:667–697.

5 Kimura S, Hara Y, Pineau T, Fernandez-Salguero P, Fox CH, Ward JM, *et al*. The T/ebp null mouse: thyroid-specific enhancer-binding protein is essential for the organogenesis of the thyroid, lung, ventral forebrain, and pituitary. Genes Dev. 1996; 10:60–69.

6 Beck-Peccoz P, Persani L, LaFranchi S. Safety of medications and hormones used in the treatment of pediatric thyroid disorders. Pediatr Endocrinol Rev 2004; 2:124–133.

7 Okamoto M, Hayase S, Miyakoshi¤b M, Murata T, Kimura S. Stem cell antigen 1-positive mesenchymal cells are the origin of follicular cells during thyroid regeneration. PLoS One 2013; 8:e80801.

8 Ornellas DS, Grozovsky R, Goldenberg R, Carvalho D, Fong P, Guggino WB, *et al*. Thyroid hormone modulates ClC-2 chloride channel gene expression in rat renal proximal tubules. J Endocrinol 2003; 178:503–512.

9 Hasebe M, Matsumoto I, Imagawa T, Uehara M. Effects of an anti-thyroid drug, methimazole, administration to rat dams on the cerebellar cortex development in their pups. Int J Dev Neurosci 2008; 26:409–414.

10 Sachidhanandam, M, Singh S, Salhan A, Ray US. Evaluation of plasma hormone concentrations using enzyme-immunoassay/enzyme-linked immunosorbent assay in healthy Indian men: effect of ethnicity. Indian J Clin Biochem 2010; 25:153–157.

11 Bancroft JD, Gamble M. *Theory and practice of histological techniques*. China: Churchill Livingstone Elsevier; 2008. 21–35.

12 Glauert AM, Lewis PR. *Biological specimen preparation for transmission electron microscopy*. United Kingdom: Princeton University Press; 2014. 80:30–45.

13 Dean, A, Dean G, Colombier D. *Epi-info version 1 for the year 2000 date basic statics and epidemiology on microcomputer*. Georgia, USA: CDC; 2000.

14 Eşmekaya MA, Seyhan N, Ömeroğlu S. 'Pulse modulated 900 MHz radiation induces hypothyroidism and apoptosis in thyroid cells: a light, electron microscopy and immunohistochemical study. Int J Radiat Biol 2010; 86:1106–1116.

15 Derwahl M, Nicula D. Estrogen and its role in thyroid cancer. Endocr Relat Cancer 2014; 21:T273–T283.

16 ElBakry RH, Tawfik SM. Histological study of the effect of potassium dichromate on the thyroid follicular cells of adult male albino rat and the possible protective role of ascorbic acid vitamin C. J Microsc Ultrastruct 2014; 2:137–150.

17 Collins WT, Capen CC. Ultrastructural and functional alterations of the rat thyroid gland produced by polychlorinated biphenyls compared with iodide excess and deficiency, and thyrotropin and thyroxine administration. Virchows Arch B Cell Pathol Incl Mol Pathol 1980; 33:213–231.

18 El-Sheikh A, Ibrahim H. 'The propolis effect on chlorpyrifos induced thyroid toxicity in male albino rats. Med Toxicol Clin Forensic Med 2017; 3:1–3.

19 Khan MA, Fenton SE, Swank AE, Hester SD, Williams A, Wolf JT. A mixture of ammonium perchlorate and sodium chlorate enhances alterations of the pitutary-thyroid axis caused by the individual chemicals in adult male F344 rats. Toxicol Pathol 2005; 33:776–783.

20 Schmidt F, Wolf R, Baumann L, Braunbeck T. Ultrastructural alterations in thyrocytes of Zebrafish (*Danio rerio*) after exposure to propylthiouracil and perchlorate. Toxicol Pathol 2017; 45:649–662.

21 Čakić-Milošević M, Korać A, Davidović V. Methimazole-induced hypothyroidism in rats: effects on body weight and histological characteristics of thyroid gland. Jugoslov Med Biohem 2004; 23:143–147.

22 Dadan J, Zbucki RŁ, Sawicki B, Winnicka MM, Puchalski ZJ. Activity of the thyroid parafollicular (C) cells in simple and hyperactive nodular goitre treated surgically-preliminary investigations. Folia Morphol (Warsz) 2003; 62:443–445.

23 Martín-Lacave I, Borrero MJ, Utrilla JC, Fernández-Santos JM, Miguel MD, Morillo J, *et al*. C cells evolve at the same rhythm as follicular cells when thyroidal status changes in rats. J Anat 2009; 214:301–309.

24 Diaz-Espineira M, Mol J, Van Den Ingh T, Van der Vlugt-Meijer R, Rijnberk A, Kooistra H. Functional and morphological changes in the adenohypophysis of dogs with induced primary hypothyroidism: loss of TSH hypersecretion, hypersomatotropism, hypoprolactinemia, and pituitary enlargement with transdifferentiation. Domest Anim Endocrinol 2008; 35:98–111.

25 Franceschi R, Rozzanigo U, Failo R, Bellizzi M, Di Palma A. Pituitary hyperplasia secondary to acquired hypothyroidism: case report. Ital J Pediatr 2011; 37:15.

26 Fierabracci A. Identifying thyroid stem/progenitor cells: 'advances and limitations. J Endocrinol 2012; 213:1–13.

27 Li L, Clevers H. Coexistence of quiescent and active adult stem cells in mammals. Science 2010; 327:542–545.

28 Thomas T, Nowka K, Lan L, Derwahl M. Expression of endoderm stem cell markers: evidence for the presence of adult stem cells in human thyroid glands. Thyroid 2006; 16:537–544.

29 Thomas D, Friedman S, Lin RY. Thyroid stem cells: lessons from normal development and thyroid cancer. Endocr Relat Cancer 2008; 15:51–58.

30 Hoshi N, Kusakabe T, Taylor BJ, Kimura S. Side population cells in the mouse thyroid exhibit stem/progenitor cell-like characteristics. Endocrinology 2007; 148:4251–4258.

31 Lin RY. New insights into thyroid stem cells. Thyroid 2007; 17:1019–1023.

32 Kuma V, Abbas AK, Fausto N, Mitchell R. The endocrine system. In: *Anirban Maitra. Robbins basic pathology*. 8th ed. Location: Philadelphia. Saunders/Elsevier; 2007.

33 Maenhaut C, Dumont JE, Roger PP, van Staveren WCG. Cancer stem cells: a reality, a myth, a fuzzy concept or a misnomer? An analysis. Carcinogenesis 2010; 31:149–158.

34 Morrison SJ, Spradling AC. Stem cells and niches: mechanisms that promote stem cell maintenance throughout life. Cell 2008; 132:598–611.